FUNDAMENTAL PREREQUISITES FOR ELECTRIC FLYING

H. Kuhn, A. Sizmann
Bauhaus Luftfahrt e.V. Lyonel-Feininger-Str. 28, 80807 Munich, Germany

Abstract

The most important challenge for the long-term future of the aviation industry is the substitution of fossil kerosene by a renewable energy base. Fully electric or hybrid-electric motive power systems have the potential to tap into a vast resource of renewable primary energy in combination with a significant reduction of emissions. This paper presents a future technology analysis approach in response to the fundamental requirements for electric flight. The Ragone metrics are applied at the component level of batteries and at the system level of hybrid-electric motive power system architectures. It is shown that (a) the advantage of hybrid power systems originates from a non-stationary power demand, (b) that the hybrid power system mass, derived from the fundamental step-function profile for a non-stationary power demand, yields a characteristic time scale for peak power demand for which a hybrid system can benefit from a high-power low-capacity subsystem, and that (c) the prospects for future lithium battery technology show potential for fully-electric (short-range) air transport. The combinatorial variety of battery cathode and anode materials, state-of-the-art advancements in battery research and the range extension enabled by a well-designed hybrid power system show where promising prospects and physical limits are for the introduction of (hybrid) electric air transport systems.

1 INTRODUCTION

The most important challenge for the long-term future of the aviation industry is its ability to transform its energy supply from fossil to renewable energy. To this end, fossil fuels must be substituted and/or novel aircraft using entirely renewable carbon-neutral energy carriers and power systems must be developed [1]. In the past decade, battery-based electric aeroplanes evolved that potentially pave the way to radically innovative power systems in aviation. A small number out of a wide variety of flying prototypes achieved serial production level. In order to demonstrate the feasibility of electric flying, mainly retrofits of small conventional aeroplanes incorporating off-the-shelf and specially designed components were built. On a larger scale, fully electric motive power systems are researched and developed as a sustainable and potentially emission-free perspective for transport aircraft, which would surpass the emission reduction targets of Flightpath 2050 and support the IATA 2050 goals. Zero in-flight emissions and potentially near-zero life-cycle emissions by the choice of a suitable primary energy source such as solar, wind, water or geothermal are strong drivers of fully electric power technology. Alternatively, hybrid-electric motive power systems using a combination of batteries and fuel cells or turbo engines may allow for a significant reduction of in-flight emissions for mid- to long-range missions [1, 2]. In this paper we present a future technology analysis and a mission-dependent scaling of hybrid-electric motive power systems that provide insight into future directions of research and development of electric air transport. In general, the usefulness of future power system technologies must be quantified in a system context with respect to their ability to meet the requirements for (electric) air transport, the top three of which are 1) to provide a sufficient power density, 2) to supply exergy density to deliver payload over a required distance and 3) to compare different power systems by a meaningful figure-of-merit in terms of economical, ecological or technical metrics.

The future technology analysis in this paper pertains to the fundamental prerequisites in that the Ragone metrics are used and the changes in hybrid power system mass are estimated based on varying requirements of peak power, cruise power and time to accomplish the mission.

For an accurate evaluation of the feasibility and perspectives of hybrid-electric motive power systems, a physics-based modelling approach of the basic components is mandatory. This paper presents a general model of the inherent power-energy interdependency (Ragone metrics) on component and system level. The Ragone metrics of an integrated power system are, similar to that of batteries, a particularly useful set of parameters for performance assessment [1, 3]. We propose a model that yields e.g. the necessary battery specific energy or the battery mass derived from mission requirements. The fundamental question concerning the prospects of the specific energy of future batteries [4] and their impact on aircraft range and payload arises as a consequence of the previous modelling approach. The next step in the future technology analysis addresses these physical bounds of the innovation potential of battery technology in order to provide a scientific basis for future electric aircraft concepts.

2 RAGONE METRICS

2.1 Ragone Diagram

The Ragone diagram, firstly introduced in 1968 to compare different battery technologies, is typically utilised to compare different electrochemical devices such as batteries and electrochemical double layer capacitors (EDLC) and displays the specific power vs. specific energy or power density vs. energy density. Specific power is related to speed or acceleration whereas the specific energy is related to range or endurance [5]. Figure 1 shows different battery technologies and their typical ranges of specific power and specific energy, adapted from [6].

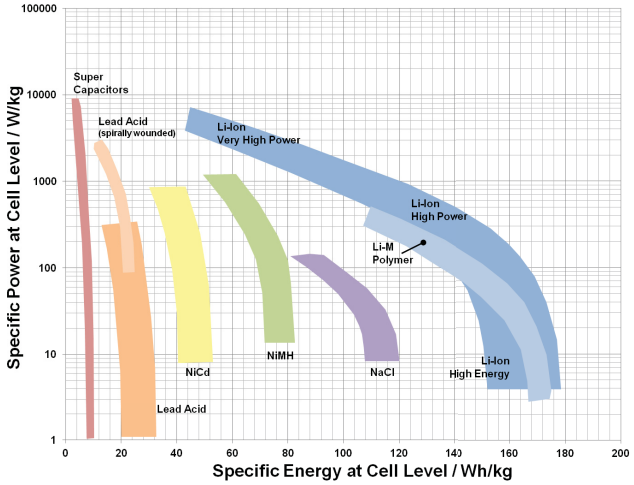

Figure 1: Ragone diagram displaying different battery technology ranges. Technology status as of 2008. Adapted from [6].

The Ragone diagram for a specific battery or electrode includes several individual measurements at various discharge currents. Available published data allows for the calculation of individual power-capacity behaviour and furthermore the power-energy behaviour on a battery level.

2.2 Ragone Diagram for Power Systems

Systems displayed within the Ragone diagram must incorporate power and energy characteristics. Energy conversion devices such as fuel cells or turbo-engines that only exhibit power characteristics would be displayed as horizontal lines intersecting the y-axis at the corresponding specific value. Energy carriers such as hydrogen or kerosene that only exhibit energy characteristics would be displayed as vertical lines intersecting the x-axis at the corresponding specific value.

Power systems comprising an energy carrier (fuel) as well as an energy converter (fuel cell or turbo-engine) can be displayed within the Ragone diagram enabling the direct comparison of different power systems [1,2]. A *relative* Ragone diagram may be established for a specific operation point of a power system, i.e. at maximum power and full fuel conditions as depicted in Figure 2, for which relevant data is given in the Appendix. To enable a meaningful comparison the system boundary is set from energy storage (fuel) to shaft power. For a todays technology level the conventional turbo-engine power system (SoA-TE) is the most powerful system available concerning maximum power and endurance[1]. A battery-based power system (Batt) enables flight (Relative Specific Power > 1) but the endurance is significant lower (Relative Specific Exergy $\ll 1$), hence the range is inacceptable low. Due to the mass penalties of additional generators and electric motors of the serial turbo-engine-electric hybrid power system (Serial-TE) the Relative Specific Power decreases to a level of ≈ 1. A reasonable range at reduced payload may be possible. The fuel cell based power system (FC) would allow for an extended endurance due to the higher specific exergy of this power system, however the Relative Specific Power is too low ($\ll 1$) to enable flight.

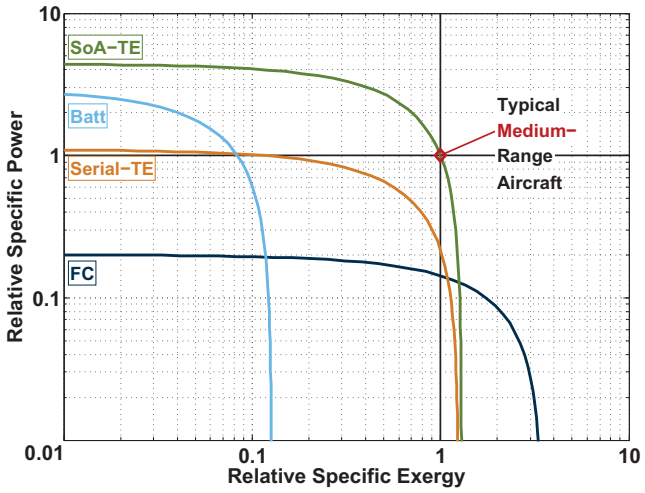

Figure 2: Relative Ragone diagram displaying different power systems normalised to a turbo-engine power system. (SoA-TE: conventional turbo-engine system; Serial-TE: serial turbo-engine-electric system; Batt: battery-based system; FC: fuel cell system)

3 ELECTROCHEMICAL ENERGY STORAGE

3.1 Required Battery Mass

For a specified time-dependent power demand, the mass of a power system scales essentially with the requirements of peak power and total mission energy. The scaling relation of power, energy and mass also fundamentally depends on the physical constraints of energy carriers and energy converters: a battery-powered system scales differently compared to a conventional fuel-powered system. The essential difference is that

[1] Included in the mass budget are: SoA-TE: fuel, tank, turbo-engine; Batt: battery, el. motor; Serial-TE: fuel, tank, turbo-engine, generator, motor; FC: hydrogen, LH_2 tank, fuel cell, balance of plant, el. motor. Power system composition is not exhaustive by purpose.

the battery is an integrated energy storage and power delivery device, where charge capacity and charge mobility at a microscopic level determine energy content and power performance. A conventional power system allows for an independent scaling of stored energy (fuel mass) and installed power (e.g. turbo-engine) on a macroscopic component and configuration level. In both cases, however, the complete power system comprising energy storage and conversion can be characterized by the Ragone metrics.

Batteries, which combine energy storage and conversion within a single device, show an interesting scaling behavior due to the inherent trade-off between power delivery and exergy content. This not only applies to the power output and exergy efficiency of a single cell, but is also evident from the typical Ragone profiles of the power-exergy envelope functions of battery technologies in Figure 1. In the following, we first present the essential modeling results for this trade-off at a single-cell level to define the critical time scale for depletion of the battery, and then use a fixed set of specific exergy and specific power variables with their associated time scale as specification of the battery to derive the essential first-approximation mass scaling. The battery mass scaling is then used as input for an analysis of mass scaling of hybrid power systems comprised of battery and fuel cell technology and the essential scaling behaviour is discussed. This approach yields a conservative (higher) mass estimate which in future work can be extended by using a linearized power-efficiency trade-off, or by using the complete analytic nonlinear relation of power and efficiency of the battery for the mass minimization of the hybrid power system, which, however, is beyond the scope of this paper.

For the basic power-efficiency modeling of batteries we assume that a maximum exergy capacity E_0 exists, from which a fraction $E_{\mathrm{ext}} < E_0$ is delivered to the external power user when the battery capacity is depleted. We further assume that the internal exergy losses $E_{\mathrm{loss}} = E_0 - E_{\mathrm{ext}}$ are due to the combined internal ohmic resistance R_i of the electrolyte, separator, electrodes and current collectors, which are valid and useful assumptions for steady-state-operation of a battery. As a result, the essence of the Ragone relation of power P_{ext} and exergy E_{ext} delivered to the external load is given by

$$P_{\mathrm{ext}}(E_{\mathrm{ext}}) = \frac{{U_0}^2}{R_i}\frac{E_{\mathrm{ext}}}{E_0}\left(1 - \frac{E_{\mathrm{ext}}}{E_0}\right), \qquad (1)$$

where U_0 is the open circuit voltage. The peak power capability of the battery is given by $P_{\mathrm{max}} = {U_0}^2/(4R_i)$. In a scaled and dimensionless representation, this relation reduces to

$$\psi_{\mathrm{ext}} = 4\,\eta_{\mathrm{batt}}\,(1 - \eta_{\mathrm{batt}}). \qquad (2)$$

which represents the essential trade-off between battery power ratio $\psi_{\mathrm{ext}} = P_{\mathrm{ext}}/P_{\mathrm{max}}$ and exergy efficiency $\eta_{\mathrm{batt}} = E_{\mathrm{ext}}/E_0$.

As a result, the battery efficiency approaches 100% only in the limit of extremely low power ratios ($\psi_{\mathrm{ext}} \to 0$), a limit in which the internal impedance is negligible compared to the external load impedance. The exergy efficiency reduces to 50% at maximum power delivery ($\psi_{\mathrm{ext}} = 1$), where thermal contraints may set a lower maximum power level or a shorter time limit than given in this model.

The time scale of power delivery until depletion is simply given by $t_d = E_{\mathrm{ext}}/P_{\mathrm{ext}} = \rho_e/\rho_p$ when E_{ext} is the maximum exergy that can be delivered at the given power level P_{ext}. In the dimensionless notation the depletion time scale is $\tau_d = t_d(E_0/P_{\mathrm{max}})^{-1} = \eta_{\mathrm{batt}}/\psi_{\mathrm{ext}}$. If the operating time t is larger than t_d, then the battery operates at reduced power level and the energy content determines the required battery size.

Hence the necessary battery mass m_{Battery} is determined by the required power P, the operating time t, energy E and the corresponding ratio of specific energy ρ_e to specific power ρ_p which is different for different operating points of a battery[2]. The battery mass is given by the following equation

$$m_{\mathrm{Battery}} = \begin{cases} P/\rho_p & t < \rho_e/\rho_p \\ \text{if} & \\ E/\rho_e & t > \rho_e/\rho_p \end{cases} \qquad (3)$$

Equation 3 determines the battery mass for steady-state operations. In a first step, a load changes can be considered as two steady-state conditions and Equation 3 applies for each steady-state condition. For dynamic load changes the current-dependent internal resistance needs to be known which is gained from polarisation curves.

3.2 Specific Energy Prospects

Batteries are the key technology for fully-electric motive power systems. Todays capacities and specific energies of lithium batteries are the highest of all current battery technologies but still insufficient for long-range automobile applications. As discussed in Section 3.1 the necessary battery mass is determined by the power and energy demand of the application. Lithium metal oxides such as lithium cobalt, lithium manganese or the emerging lithium iron phosphates are the most utilised positive electrode materials for commercial batteries exhibiting theoretical capacities of less than 170 mAh/g in the charged state [7, 8]. Graphite is still the state-of-the-art negative electrode material with a practical capacity of 350 mAh/g. Hence, utilising standard electrode materials commercial batteries are limited to specific energies of less than 300 Wh/kg. Due to improvement of electrode and electrolyte structure

[2] Three operating conditions may be used as reference points of Eq. 2, the high-efficiency case with $\eta_{\mathrm{batt}} = 90\%$ at a power level of $\psi_{\mathrm{ext}} = 36\%$ and $\tau_d = 2.5$, the half-maximum power level ($\psi_{\mathrm{ext}} = 50\%$) at $\eta_{\mathrm{batt}} = 85\%$ and $\tau_d = 1.7$, and a balanced high-power regime of $\psi_{\mathrm{ext}} = 75\%$ and $\eta_{\mathrm{batt}} = 75\%$ with $\tau_d = 1$.

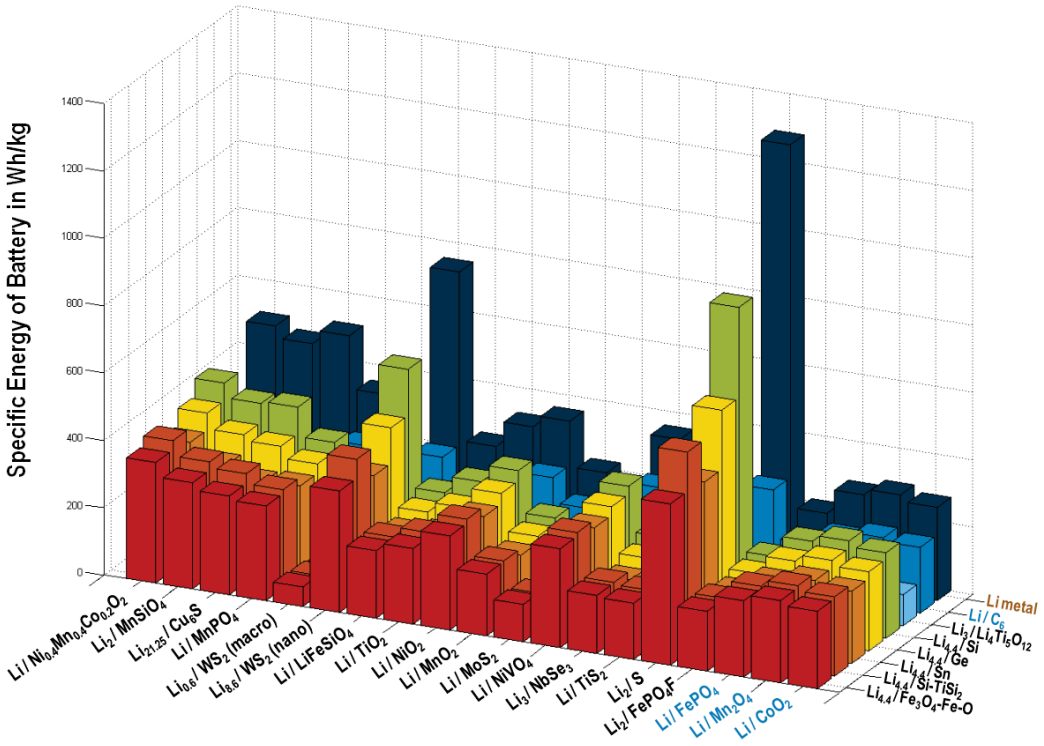

Figure 3: Compilation and results of a combinatorial battery analysis of recently discussed positive and negative electrode materials. State-of-the-art electrode materials for secondary lithium batteries are highlighted in blue.

commercial batteries show specific energies of up to 245 Wh/kg at a discharge rate of 0.2 C which translates to a specific power of 49 W/kg. The same battery is also cabaple of delivering 237 Wh/kg at a discharge rate of 1 C (ρ_p = 237 W/kg) [9].

Today batteries are optimised for either high power or high energy densities which is realised by proper electrode morphology and electrolyte. Future nano-structured electrode materials may overcome this limitation due to short diffusion paths of the ions.

Beside the electrodes and electrolyte a battery comprises non-electrochemical parts such as current collectors, separator, housing, etc. which reduces the overall specific energy on battery level. An optimum limit concerning the non-electrochemical parts is reached [10]. To enhance power and durability of batteries new electrode materials are strongly required and are the key for significant improvements. Various positive as well as negative electrode materials are investigated to further improve lithium battery characteristics. In order to determine the potential of future battery specific energies several electrode materials are analysed with respect to equilibrium potential vs. Li/Li^+, molar mass and reversible range from original scientific publications to readily calculate potential theoretical specific energies [4]. Figure 3 shows the theoretical specific energies on battery level of the investigated electrode combinations. State-of-the-art electrode materials are highlighted in blue. Lithium metal as negative electrode material exhibits for all combinations the highest specific energy but is not used in commercial rechargeable lithium cells due to safety risks arising from dendrite build-up and short-circuiting leading to thermal runaway of the cell.

From Figure 3 most promising negative electrodes are for example silicon (Si), germanium (Ge), tin (Sn) and nano-structured titanium-supported silicon. Sulphur (S), nano-structured tungsten disulfide (WS_2) and nickel-manganese-cobalt metal oxides ($Ni_yMn_yCo_{1-2y}O_2$) are most promising positive electrode materials. Specific energies on battery levels of these combinations are well above 300 Wh/kg but still less than 1000 Wh/kg.

Lithium-air batteries are often discussed and specific energies up to 11500 Wh/kg are stated. This highly misleading number neither takes into account all reactants nor the electrolyte, separator, current collectors, housing, structure of the positive electrode (gas diffusion electrode, catalyst, binder) etc. Accounting for these parts as well as necessary excess lithium due to lithium loss during cycling the practical specific energy of lithium-air batteries is around 600-630 Wh/kg, 2-3 times the specific energy of commercial lithium batteries today [11–13] showing the same order of magnitude as for lithium-sulphur cells [11].

3.3 Specific Power Prospects

For safety reasons lithium intercalation electrodes are utilised in commercial lithium batteries instead of lithium metal for more than 20 years. That means lithium ions from the electrolyte diffuse into and out of the bulk electrode material. This diffusion process is the rate determining step limiting the power capabilities of lithium batteries. In order to reduce ion diffusion lengths downsizing of the electrode structures from micro to nano-structures or electrode coatings result in a significant improvement of ion exchange rate capabilities.

Kang and Ceder demonstrated very high exchange rates for coated $LiFePO_4$ positive electrode materials which are utilised as electrode materials in the recent years [14]. They applied a lithium phosphate coating onto nano-scale $LiFePO_4$. The theoretical capacity of the electrode material is ~166 mAh/g which is even achieved at a discharge rate as high as 2 C[3]. At a discharge rate of 50 C (full discharge in 72 s) still ~80 % of the theoretical capacity is gained. With the lithium phosphate coating capacities as high as 120 mAh/g for a 200 C rate (full discharge in 18 s) and 60 mAh/g for a 400 C rate (full discharge in 9 s) are demonstrated. Typical specific powers of lithium batteries today are in the range of 0.5 to 2 kW/kg whereas the lithium phosphate coated $LiFePO_4$ exhibits specific powers of 90 to 170 kW/kg at 200 and 400 C, respectively. Kang and Ceder state that with such kind of electrodes 180 kW are required to charge a 15 kWh battery within 5 minutes.

The specific power of reported lithium-air batteries is in the range of mW/kg, which is 1/100 of that of commercial lithium batteries [11, 13, 15, 16]. According to Equation 3, the resulting overall battery mass would be prohibitively high. Due to the very low power capabilities we do not consider lithium-air batteries as a viable technology for aviation applications.

3.4 Supercapacitor Prospects

Compared to batteries electrochemical double layer capacitors (EDLC[4]) exhibit very high power capabilities as high as 20 kW/kg but insufficient specific energies below 6 Wh/kg [17] based on porous carbon electrodes and aqueous electrolytes. Because of the energy storing mechanism, the energy is stored in the electric field at the electrode-electrolyte interface, a high surface area is mandatory. Nano-structuring of the electrodes significantly increases the surface-to-volume ratio and hence the storage capacity. Lu *et al.* demonstrated very high capacities as well as high charge/discharge rates for aligned carbon nano-tubes as electrodes and an ionic liquid electrolyte. Based on the electrode masses they achieved specific energies up to 100 Wh/kg at 110 kW/kg and maximum values as high as 148 Wh/kg (at 20 kW/kg) and 315 kW/kg (at 90 Wh/kg).

The self-discharge rate of EDLC is rather high compared to batteries and is in the range of a few hours to days depending on the electrolyte [18]. Furthermore the voltage drops to zero upon discharge compared to a stable and in some cases constant voltage for batteries.

4 HYBRID POWER SYSTEMS

Hybrid power systems comprise at least two or more energy carriers *and/or* two or more energy conversion devices. A variety of hybrid power systems are investigated for automobile drive trains but a fundamental understanding of the characteristics and scaling behaviour of hybrid power systems is especially required for aviations motive power systems in order to identify promising future power systems to reduce for example the impacts regarding weight, emissions, noise, maintenance etc.

The focus of this paper are fuel cell-battery hybrid power systems and its general characteristics and limitations under two different load demands. However, the generalised method and processes are also applicable to hybrid power systems comprising different energy carriers and conversion devices.

4.1 Time-Constant Power Demand

Figure 4 shows a time-constant power demand. A hybrid power system exhibits no benefits in terms of minimising total power system mass which is shown in the next section in more detail. The minimum power system mass has the general dependency shown in Figure 5 and is characterised by the times t_a and t_b.

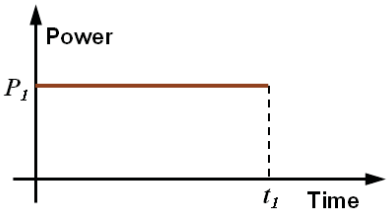

Figure 4: Time-constant power demand.

For a specific battery type and according to Equation 3 the total power system mass is constant in the time range $t < t_a = t_d$ (P) where t_d is the depletion time. Within this time range power-optimised batteries may exhibit a mass benefit due to the low energy requirements. At $t_a < t < t_b$ the battery mass increases linearly according to the energy demand (E) whereas the full power capabilities of the battery are not required. At $t > t_b$ fuel cell systems (FC) exhibit the lowest power system mass due to the high specific energy of hydrogen. Energy conversion devices and other components account for a mass offset even at $t = 0$, see Equation 4.

[3] Standard discharge rate is 0.2 C corresponding to a full discharge in 5 h.

[4] Also known as supercapacitors, ultra-capacitors, etc.

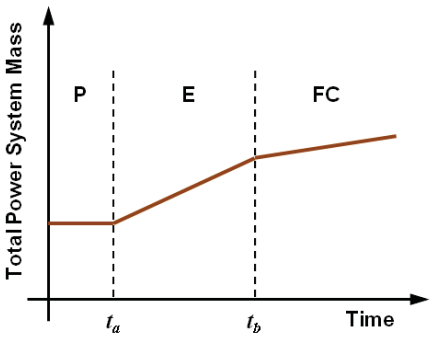

Figure 5: General behaviour of the minimum total power system mass for a power demand shown in Figure 4.

Times t_a and t_b are governed by the ratios of specific energy to specific power ρ_e/ρ_p of the considered batteries and the lower battery mass is given according to Equation 3 as well as the specific power of the fuel cell system including hydrogen storage.

4.2 Step-Profile Power Demand

For the step-profile power demand shown in Figure 6 the power management can principally be split-up into different cases. Within this article we focus on the case wherein the difference in power demand ΔP is provided by the battery at $0 \leq t \leq t_1$ whereas the fuel cell provides the power P_2 between $0 \leq t \leq t_2$. It is obvious that a subsystem adding a mass penalty is only feasible for providing temporarily surplus power (ΔP), hence a battery-based subsystem solely providing the power P_1 would exhibit a mass penalty to the overall system. Recharging the batteries within the time range $t_{\text{charge}} \leq t_2 - t_1$ opens new degrees of freedom to system optimisation and is treated in a following article.

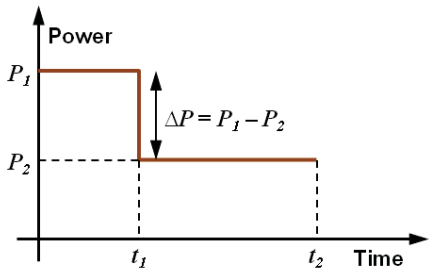

Figure 6: Step-profile power demand.

For a general discussion we introduce the power ratio $\psi = P_2/P_1$ and the time ratio $\tau = t_1/t_2$. The total hybrid power system mass is then given by the general equation

$$m = P_1 \left(\underbrace{\sum_i \frac{1}{\rho_{p,i}}}_{\alpha} + \underbrace{\sum_j \frac{\psi}{\rho_{p,j}}}_{\beta} + \underbrace{\sum_k \frac{(1-\psi)\cdot\tau\cdot t_2}{\rho_{e,k}}}_{\gamma} + \underbrace{\sum_l \frac{\psi\cdot t_2}{\rho_{e,l}\cdot\eta_l}}_{\delta} \right) + F(P_1, t_2, \psi, \tau) \quad (4)$$

where α and β are the sum of components governed by the power levels $P_{1,2}$ and the corresponding specific powers ρ_p (e.g. el. motor, power electronics, fuel cell, engine, etc.), γ is the sum of components governed by the energy demand within the time interval $0 < t \leq t_1$ providing the power demand ΔP (e.g. battery, fuel, etc.), δ is the sum of components governed by the energy demand within the time interval $0 < t \leq t_2$ providing the power demand P_2 (e.g. battery, fuel, etc.). Function F describes additional components necessary for the power system such as fuel tanks (e.g. for kerosene or hydrogen) or structural components that size with power or energy storage.

For the considered battery-fuel cell hybrid power system the power ratio $\psi \in [0 \ldots 1]$ also describes the degree of hybridisation and the following relations describe the interdependency of the two power supplying subsystems

$$\psi = \frac{P_2}{P_1} = \frac{P_2}{\Delta P + P_2} \quad (5)$$

$$P_2 = \psi P_1 \quad (6)$$

$$\Delta P = (1-\psi)\cdot P_1 \quad (7)$$

The derivatives with respect to ψ and τ are

$$\frac{\delta m}{\delta \psi} = P_1 \left(\sum_j \frac{1}{\rho_{p,j}} - \sum_k \frac{\tau\cdot t_2}{\rho_{e,k}} + \sum_l \frac{t_2}{\rho_{e,l}\cdot\eta_l} \right) + \frac{\delta F(P_1, t_2, \psi, \tau)}{\delta \psi} \quad (8)$$

$$\frac{\delta m}{\delta \tau} = P_1 \left(\sum_k \frac{(1-\psi)\cdot t_2}{\rho_{e,k}} \right) + \frac{\delta F(P_1, t_2, \psi, \tau)}{\delta \tau} \quad (9)$$

The gradient for $\delta m/\delta\tau$ is always positive because $\psi < 1$ indicating that a hybrid power system for a time-constant power demand is not favourable, see preceding section. However, the gradient for $\delta m/\delta\psi$ may change from positive to negative for $\tau \to 1$ indicating that for certain conditions depending on the component specific power ρ_p characteristics the mass of the fuel cell-battery hybrid power system may be minimised compared to a pure fuel cell or battery based system.

The general Equation 4 applied to a fuel cell-battery hybrid power system according to Case 1 reads as

$$m_{\text{HPS}} = P_1 \left(\frac{1}{\rho_{p,\text{mot}}} + \frac{1}{\rho_{p,\text{pmad}}} + \frac{(1-\psi)\cdot\tau\cdot t_2}{\rho_e} + \frac{\nu\cdot\psi}{\rho_{p,\text{fc}}} + \frac{\psi\cdot t_2}{\rho_{e,\text{LH2}}\cdot\eta} \right) + F(P_1, t_2, \psi) \quad (10)$$

where ν accounts for additional mass for the balance of plant of the fuel cell system.
The first line accounts for the electric motor and power electronics that size with maximum power demand and the corresponding specific powers ρ_p. The second line accounts for the battery mass depending on the power ratio ψ, the time ratio τ and specific energy of the battery ρ_e. The third line accounts for the fuel cell comprising the fuel cell system, hydrogen and hydrogen tank. The general behaviour of the total system mass for a fuel cell-battery hybrid power system is shown in Figure 7. The total mass is according to Equation 4 sizing with the maximum power demand P_1.

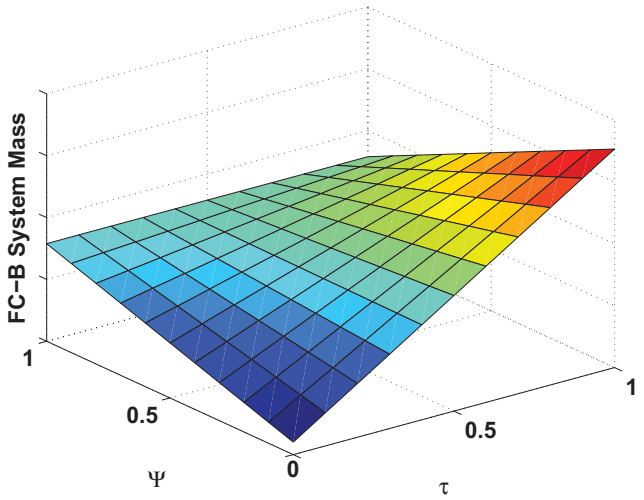

Figure 7: General behaviour of the total system mass of a fuel cell-battery hybrid power system depending on ψ and τ.

Applying $\delta m_{\mathrm{HPS}}/\delta\psi = 0$ yields τ_0 where $\delta m/\delta\psi$ changes the algebraic sign from positive to negative for increasing τ. At $\tau > \tau_0$ a mass benefit arises for the battery-fuel cell hybrid power system. τ_0 is approximately characterised by

$$\tau_0 \approx \frac{\rho_e}{t_2}\left(\frac{\nu}{\rho_{p,\mathrm{fc}}} + \frac{t_2}{\rho_{e,\mathrm{LH2}}\cdot\eta}\right) \qquad (11)$$

τ_0 is governed by the specific power and specific energy characteristics of the employed components as well as the overall time t_2.

In order to compare the specific mass of different hybrid power systems the maximum power level P_1, the maximum operation time t_2, the power ratio as well as the time ratio ψ and τ, respectively, needs to be determined.

5 SUMMARY

In this paper, the fundamental requirements for electric flight were presented and applied to battery performance and to the hybrid power systems. Identified as a fundamental prerequisite for electric flying, lithium battery technology was analysed with respect to its future potential. The total mass scaling of a hybrid-electric power system for varying power demand was evaluated in a basic linear framework for transparency of its overall behaviour.

The critical assessment of the requirements for electric aviation builds on the previously defined three fundamental principles of feasibility assessment for electric flying [1, 3], i.e. on the significance of (1) the specific exergy content rather than energy content of an energy carrier, (2) the Ragone metrics and (3) the hybridization degree of freedom. The Ragone metrics are essential to evaluate the specific power and specific energy requirements (e.g. the technology gap relative to a conventional aircraft or a new concept) and hybridisation offers a degree of freedom for a technology mix and system design to satisfy both peak power and mission energy demands.

In this paper it was shown that (a) the advantage of hybrid power systems originates from a non-stationary power demand, (b) that the hybrid power system mass, derived from the fundamental step-function profile for a non-stationary power demand, yields a characteristic time scale for peak power demand for which a hybrid system can benefit from a high-power low-capacity subsystem, and that (c) the prospects for future lithium battery technology show potential for improvement for application in electric (short-range) air transport.
The characteristic time scale for peak power demand has been modeled using a step-function of piecewise stationary peak power and cruise power demand as a basic mission profile. The hybridisation degree of freedom of the battery-fuel cell combination was locked to the power profile by assuming that the extra power required above cruise power demand is supplied by the batteries.

It is straightforward to extend this analysis to a linearised power-efficiency trade-off or to include the exact non-linear mass scaling. As indicated in the paper, greater detail in physical modeling of power-exergy-mass relations of hybrid power system components, to replace fixed specifications of such devices, will reproduce the essential behaviour of the linear framework with a more accurate and more favourable mass scaling, which is subject of future work.

Another future direction is to compose and optimize hybrid-eletric power system architectures to best match the characteristics of mission profiles in order to maximise the performance benefits measured in system mass, efficiency, emissions etc., and to include operational degrees of freedom such as recharging of batteries during flight to reduce the fuel weight. As a first step, the optimisation of the hybridisation degree of freedom for a given mission was presented in a recent study [2].

As a key enabler of electric flight, lithium battery technology has been modeled in a combinatorial variety of cathode and anode materials, and the weight penatlies for essential non-electro-chemical components have been

included. This future technology assessment showed (a) that a two- to three-fold increase in capacity is plausible and scientific progress and technological innovation in the fields of nano-structured energy materials is essential to close the technology gap between requirements and performance of power systems for electric aviation, and (b) that the range extension of electric aircraft requires a well-designed hybrid power system with a non-battery high-energy density subsystem with specifications beyond the limits of lithium battery technology.

References

[1] H. Kuhn, C. Falter, A. Sizmann. *Renewable Energy Perspectives for Aviation*. Proceedings of the 3^{rd} CEAS Air&Space Conference and 21^{st} AIDAA Congress, Venice, Italy, pp. 1249-1259 (2011).

[2] H. Kuhn, A. Seitz, L. Lorenz, A.T. Isikveren, A. Sizmann. *Progress and Perspectives of Electric Air Transport*. 28^{th} Int. Congress of the Aeronautical Sciences, Brisbane, Australia, 2012, ID 947, accepted.

[3] A. Sizmann. *Neue Energieperspektiven der Luftfahrt*. Fuelling the Climate 2010, Hamburg, Germany, 2010, http://www.haw-hamburg.de/ftz-als/veranstaltungen/veranstaltungsarchiv/klimaschutz-in-der-luftfahrt0.html.

[4] H. Kuhn. to be published.

[5] D.V. Ragone. *Review of Battery Systems for Electrically Powered Vehicles*. SAE Technical Paper 680453 (1968).

[6] U. Köhler. *Battery Systems for Smart Electric Vehicles*. EPoSS Seminar, Brussels, Belgium, 2008.

[7] M. Winter, J.O. Besenhard, M.E. Spahr, P. Novák. *Insertion Electrode Materials for Rechargeable Lithium Batteries*. Adv. Mater. **10**(10), pp. 725-763 (1998).

[8] M.S. Whittingham. *Lithium Batteries and Cathode Materials*. Chem. Rev. **104**(10), pp. 4271-4301 (2004).

[9] Panasonic Lithium-Ion Battery NNP-Series, Type NCR-18650-A, February 2010.

[10] B. Scrosati, J. Garche. *Lithium batteries: Status, prospects and future*. J. Power Sources **195**(9), pp. 2419-2430 (2010).

[11] P.G. Bruce, S.A. Freunberger, L.J. Hardwick, J.M. Tarascon. *Li-O2 and Li-S batteries with high energy storage*. Nature Materials **11**(1), pp. 19-29 (2012).

[12] Y. Wang, H. Zhou. *A lithium-air battery with a potential to continuously reduce O2 from air for delivering energy*. J. of Power Sources 195(1), pp. 358-361 (2010).

[13] A. Kraytsberg, Y. Ein-Eli. *Review on Li-air batteries: Opportunities, limitations and perspective*. J. of Power Sources 196(3), pp. 886-893 (2011).

[14] B. Kang, G. Ceder. *Battery materials for ultrafast charging and discharging*. Nature **458**(7235), pp. 190-193 (2009).

[15] T. Kuboki, T. Okuyama, T. Ohsaki, N. Takami. *Lithium-air batteries using hydrophobic room temperature ionic liquid electrolyte*. J. Power Sources 146(1-2), pp. 766-769 (2005).

[16] J.G. Zhang, D. Wang, W. Xu, J. Xiao, R.E. Williford. *Ambient operation of Li/Air batteries*. J. Power Sources 195(13), pp. 4332-4337 (2010).

[17] Maxwell Technologies, Inc., San Diego (CA), USA, K2 Series Ultracapacitors, www.maxwell.com.

[18] A.B. Fuertes, G. Lota, T.A. Centeno, E. Frackowiak. *Templated mesoporous carbons for supercapacitor application*. Electrochimica Acta **50**(14), pp. 2799-2805 (2005).

APPENDIX

Table 1 summarises characteristic component values of 2010 applied for the calculation of the relative Ragone diagram in Figure 2 as well as expected values in the future.

Table 1: Characteristic values for the power system components [2].

Component	Unit	2010	2035+
Kerosene	kWh/kg	11.9 [a]	
Hydrogen (LH_2)	kWh/kg	33.31 [a]	
Fuel tank	kg	– [b]	
Lithium battery	kWh/kg	0.60	1.0
Turbo-engine[c]	kW/kg	15.0	18.0
Fuel cell (PEFC) [d]	kW/kg	1.2	3.0
Percentage of BoP [e]		0.50	0.30
Generator	kW/kg	10.0	30.0
Motor	kW/kg	10.0	30.0
Power management[f]	kW/kg	10.0	20.0
Efficiencies		**2010**	**2035+**
Turbo-engine		0.50	0.55
Fuel cell		0.50	0.65
Generator		0.99	0.99
Motor		0.99	0.99
Power management		0.95	0.98

[a] Lower Heating Value (LHV)
[b] The mass of the fuel tanks are calculated separately depending on the fuel amount.
[c] bare turbo-shaft specific power at max power
[d] PEFC: Polymer Electrolyte Fuel Cell
[e] BoP: Balance of Plant
[f] single system without redundancies